Frontiers in Bioscience Landmark

Front. Biosci. (Landmark Ed) **2022**; 27(10): 298
https://doi.org/10.31083/j.fbl2710298

Original Research

Human Urinary Kallidinogenase Pretreatment Inhibits Myocardial Inflammation and Apoptosis after Coronary Microembolization by Activating PI3K/Akt/FoxO1 Axis

Jian Xie[1,†], Binhai Mo[2,†], Yunhua Lin[3], Guoqing Liu[3], Qingqing Nong[3], Bingling Wu[3], Yuqian Xie[3], Tao Li[1], Lang Li[1,4,5,*]

[1]Department of Cardiology, The First Affiliated Hospital of Guangxi Medical University, Guangxi Cardiovascular Institute, 530021 Nanning, Guangxi, China
[2]Department of Cardiology, The First People Hospital of Nanning & The Fifth Affiliated Hospital of Guangxi Medical University, 530016 Nanning, Guangxi, China
[3]The First Clinical College, Guangxi Medical University, 530021 Nanning, Guangxi, China
[4]Guangxi Key Laboratory of Precision Medicine in Cardio-Cerebrovascular Diseases Control and Prevention, 530021 Nanning, Guangxi, China
[5]Innovative Research Team of Guangxi Natural Science Foundation, 530021 Nanning, Guangxi, China
*Correspondence: drlilang1968@126.com (Lang Li)
[†]These authors contributed equally.

Academic Editor: Graham Pawelec
Submitted: 18 July 2022 Revised: 28 August 2022 Accepted: 6 September 2022 Published: 31 October 2022

Abstract

Background: As a fatal cardiovascular complication, coronary microembolization (CME) results in severe cardiac dysfunction and arrhythmia associated with myocardial inflammation and apoptosis. Human urinary kallidinogenase (HUK) can provide a protective function for cardiomyocytes by improving microcirculation. However, the therapeutic effects and underlying mechanisms of HUK in CME-induced myocardial injury remain unclear. **Aims**: We evaluated the effect of HUK on cardiac protection in a rat model of CME and whether it could restrain myocardial inflammation and apoptosis, and alleviate CME-induced myocardial injury. **Methods**: We established the CME model by injecting 42 μm inert plastic microspheres into the left ventricle of rats in advance, then the rats were randomly and equally divided into CME, CME + HUK (the dose of HUK at 0.016 PNA/kg/day), CME + HUK + LY (the dose of LY294002 at 10 mg/kg, 30 minutes before modeling), and Sham operation groups. Cardiac function, the serum levels of myocardial injury biomarkers, myocardial inflammation and apoptosis-related genes were measured; and the myocardial histopathological examination was performed at 12 h after the operation. **Results**: The results revealed that HUK effectively reducing myocardial inflammation, apoptosis, and myocardial infarction area; and improving CME-induced cardiac injury by activating the PI3K/Akt/FoxO1 axis. In addition, these cardioprotective effects can be reduced by the PI3K specific inhibitor LY294002, suggesting that the aforementioned protective effects may be related to activation of the PI3K/Akt/FoxO1 axis. **Conclusions**: HUK seems to control inflammatory infiltration and cardiomyocyte apoptosis significantly to improve CME-induced cardiac injury via regulating the PI3K/Akt/FoxO1 axis.

Keywords: human urinary kallidinogenase; coronary artery microembolization; PI3K/Akt/FoxO1; myocardial inflammation; apoptosis

1. Introduction

Coronary artery microembolization (CME) is a major cause of "no recurrent flow" in occluded coronary arteries after interventional procedures [1,2]. It is considered to be the main complication of percutaneous coronary intervention (PCI) [3]. CME may disrupt myocardial reflow, leading to severe cardiac dysfunction and arrhythmia [4]. Moreover, a study by Heusch *et al.* [5] indicated that repetitive CME could cause progressive loss of functional cardiomyocytes and induce heart failure. Rat CME has also been reported to display a local myocardial infarction, with a large number of apoptotic and necrotic cells in the corresponding area [6]. Therefore, existing studies indicate that myocardial inflammation and apoptosis may play vital roles in CME-induced myocardial damage, and targeted interventions in these aspects might be critical for myocardial protection [7–9].

Recently, the potential protective mechanism of the PI3K/Akt axis in CME has received considerable attention. For example, gustazine has been shown to inhibit oxidative stress and inflammation by influencing the PI3K/Akt pathway, thereby reducing myocardial damage caused by CME in rats [10]. Human urinary kallidinogenase (HUK), a glycoprotein found in male urine that modulates the kallikrein-kinin system, has been used in a wide range of patients diagnosed with ischemic stroke [11]. Ma *et al.* [12] confirmed that HUK acts as an anti-inflammatory and anti-apoptotic factor through the PI3K/Akt/FoxO1 signaling pathway, thereby reducing brain damage in rats with persistent middle cerebral artery occlusion. However, further research is required to confirm whether HUK can reduce myocardial damage caused by CME and improve car-

Fig. 1. The flow chart of our study.

diac function through the PI3K/Akt/FoxO1 signaling pathway. This study aimed to explore the effect of HUK on myocardial inflammation and apoptosis and its role in the PI3K/Akt/FoxO1 pathway to determine whether it improves CME-induced cardiac dysfunction and increases cardiac output.

2. Materials and Methods

2.1 Grouping and CME Model Establishment

The flow of our study was represented in Fig. 1. All experimental animals were procured from the Experimental Animal Center of Guangxi Medical University. All experimental protocols and steps according to the NIH (National Institutes of Health) Guidelines for the Use of Laboratory Animals, and had the approval of the Animal Ethics Committee. Firstly, 40 male adult Sprague-Dawley (SD) rats of 250–300 g were randomly divided into CME, CME + HUK treatment, CME + HUK + LY, and sham operation groups, with ten rats in each group. We then built a CME model based on the previously reported process [9]. Briefly, an intraperitoneal injection of pentobarbital sodium (30–40 mg/kg) was administered to anesthetize the SD rats. We used a small-animal ventilator to assist with breathing. We conducted a left-sided thoracotomy in the incision position between the third and fourth ribs of the rat. The ascending aorta was separated and gripped for 10 s. Simultaneously, we mixed 3000 plastic microspheres of 42 μm diameter (BioSphere Medical Inc., USA) in 0.1 mL sodium lauryl sulfate, which were injected into the left ventricle via the apical part of the heart. An equal volume of saline was injected into the Sham group in the same way. The CME + HUK and CME + HUK + LY groups were administered HUK 0.016 PNA/kg via tail vein for seven consecutive days prior to surgery [13,14]. And the CME + HUK + LY group was given 10 mg/kg LY294002 (a specific inhibitor of PI3K) (APExBIO, Houston, USA) preoperatively via the peritoneal cavity for 30 min [15]. Penicillin was applied to all animals to resist infection.

2.2 Cardiac Function Measurements

Based on Chen *et al.* [4] study, 12 hours after modeling is the best time to measure cardiac function in rats while at the lowest level. At that stage, we evaluated the cardiac function of the rat using the Hewlett-Packard Sonos (Philips Sonos7500 system, Philips Technologies, USA) to measure the left ventricular fraction shortening (LVFS), left ventricular ejection fraction (LVEF), left ventricular end-systolic diameter (LVESd), and left ventricular end-diastolic diameter (LVEDd), respectively. The measurement was repeated thrice for each rat, and the average value was calculated. All the above operations were performed using an S12 probe with a 12 MHz probe. Experienced cardiac sonographers were used to perform all ultrasound examinations.

2.3 Serum cTnI\CK-MB\LDH\IL-1β\TNF-α Measurement Using Enzyme-Linked Immunosorbent Assay

Blood samples were drawn from the abdominal aorta before sacrifice. The levels of serum cardiac troponin I (cTnI), creatine kinase myocardial band isoenzyme (CK-MB), lactate dehydrogenase (LDH), IL-1β, and TNF-α were estimated using enzyme-linked immunosorbent assay (ELISA) according to the manufacturer's instructions. All the above tests were performed using standardized ELISA kits (Bio-Swamp Biological Technology Co., Ltd., USA).

2.4 Sample Collection and Processing

Twelve hours after the operation, the rats were sacrificed for sampling after completing the ultrasound examination. We administered an intraperitoneal injection of pentobarbital sodium (60 mg/kg) to anesthetize rats. Blood was collected from the abdominal aorta and the heart was isolated shortly after opening the chest. The auricle and atrium were then excised, and the cardiac tissue was separated into upper, middle, and bottom sections. For the comparability of each group, the same inspection index was performed using the same part of cardiac tissue. The upper and middle sections were kept at –80 °C to prepare for real-time quantitative PCR (RT-qPCR) and western blotting. The bottom sections were immobilized in 4% paraformaldehyde for 12 h. It was then embedded in paraffin and used for slice preparation. After hematoxylin-eosin (H&E) staining, cardiomyocytes were observed after CME using an optical microscope. Hematoxylin-basic fuchsin-picric acid (HBFP) staining was used to identify myocardial ischemia, and terminal deoxynucleotidyl transferase dUTP nick end labeling (TUNEL) staining was used to identify cardiomyocyte apoptosis.

2.5 Detection of Myocardial Microinfarction Area

Myocardial ischemia was detected via HBFP staining, which enabled the staining of ischemic cardiomyocytes and

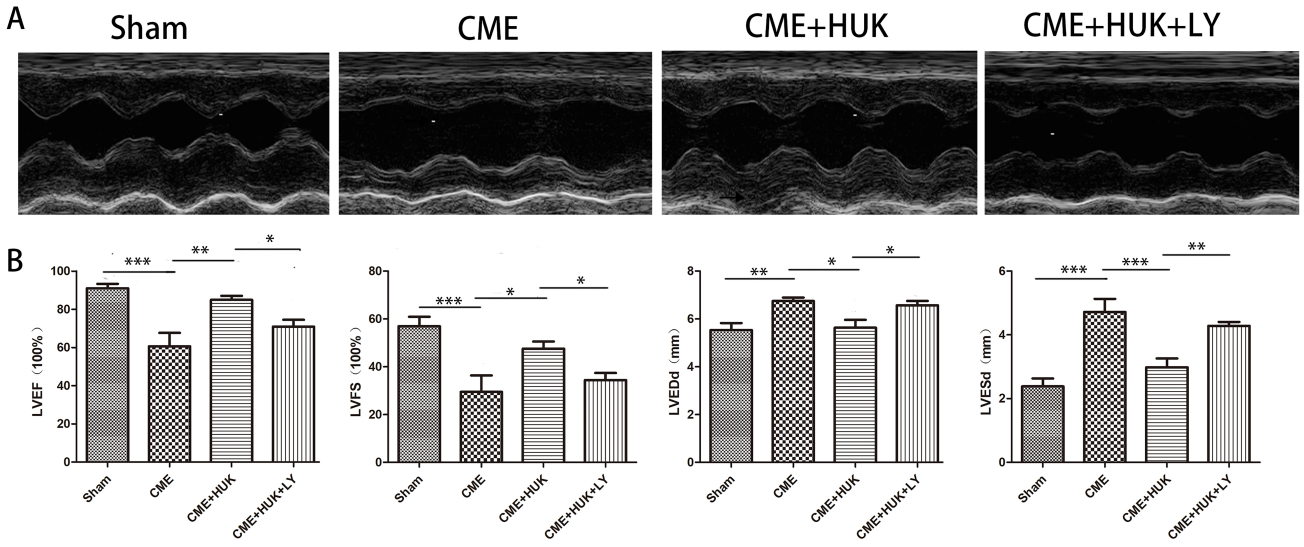

Fig. 2. Measurement of cardiac function. (A) Cardiac function evaluated by echocardiography in each group (n = 6, per group). (B) The cardiac function parameters of left ventricle ejection fraction (LVEF), left ventricle fractional shortening (LVFS), left ventricular end-diastolic diameter (LVEDd), and left ventricular end-systolic diameter (LVESd) were measured quantitatively. Data were presented as the mean ± standard deviation (SD). *$p < 0.05$, **$p < 0.01$, ***$p < 0.001$. Abbreviations: CME, coronary microembolization; HUK, Human Urinary Kallidinogenase; LY, LY294002.

cytoplasm (red), and the nuclei of infarcted (yellow) and healthy (blue) cardiomyocytes. Each stained section was observed with a pathology image analyzer (DMR + Q550, Leica, Wetzlar, Germany). Five fields of view were obtained from each slice. Leica Qwin software (2.7, Leica Microsystems Inc, Buffalo Grove, IL, USA) and the planar method were used to calculate the infarct area. The infarct area was then divided by the entire observation area to measure the infarct percentage.

2.6 Detection of Cardiomyocyte Apoptosis

The TUNEL assay (Roche, USA) was performed using a TUNEL apoptosis detection kit according to the manufacturer's instructions to detect cardiomyocyte apoptosis. The nuclei of apoptotic cells appeared yellowish-brown under light microscopy. Forty nonoverlapping regions were randomly selected from each slice (×400 magnification). The total number of apoptotic and normal cardiomyocytes was counted. The number of apoptotic cardiomyocytes was obtained using the formula of the count of apoptotic cardiomyocytes/gross count of cardiomyocytes.

2.7 Immunofluorescence Staining

We prepared slices of 4 μm thickness and performed immunofluorescence (IF) staining using the manufacturer's instructions, following which the slices were incubated with the three antibodies (cleaved caspase-3 [#9661, Cell Signaling Technologies, Danvers, MA, USA], Bax [ab53154, Abcam, Cambridge, UK], and Bcl-2 [ab194583, Abcam]) at 4 °C overnight. PBS was used to rinse the slices five times after incubation with primary antibodies. The slices were then incubated with fluorescent secondary antibodies for 50 min at room temperature. Subsequently, images of 4',6-diamidino-2-phenylindole (DAPI) counterstained cell nuclei for 7 min were acquired with a fluorescence microscope (Olympus, Tokyo, Japan).

Table 1. Sequences of the used primers for RT-qPCR.

GENE	NCBI ID	Primer Sequence
Bcl-2	24224	Forward: 5′-CCTGGCATCTTCTCCTTCCA-3′ Reverse: 5′-GGACATCTCTGCAAAGTCGC-3′
Bax	24887	Forward: 5′-AAGAAGCTGAGCGAGTGTCT-3′ Reverse: 5′-CCAGTTGAAGTTGCCGTCTG-3′
Caspase-3	25402	Forward: 5′-TGTCGATGCAGCTAACCTCA-3′ Reverse: 5′-GCAGTAGTCGCCTCTGAAGA-3′
GAPDH	24383	Forward: 5′-TGTGAACGGATTTGGCCGTA-3′ Reverse: 5′-GATGGTGATGGGTTTCCCGT-3′

2.8 Real-time Quantitative PCR

Samples of heart tissue (200 mg) were processed by RT-qPCR. Following the manufacturer's instructions, we extracted apoptosis-associated RNAs such as Bax, Bcl-2, and caspase-3, which were determined by RT-qPCR for relative levels in CME. The ABI PRISM-7500 machine (CA, USA) was used to perform RT-qPCR using the TB Green® Premix Ex Taq™ II (TaKaRa, Japan). The specific primer sequences used in this study were listed in Table 1.

2.9 Western Blotting

Sodium dodecyl sulfate polyacrylamide gel electrophoresis (SDS-PAGE) (stacking gel: 5% SDS-PAGE,

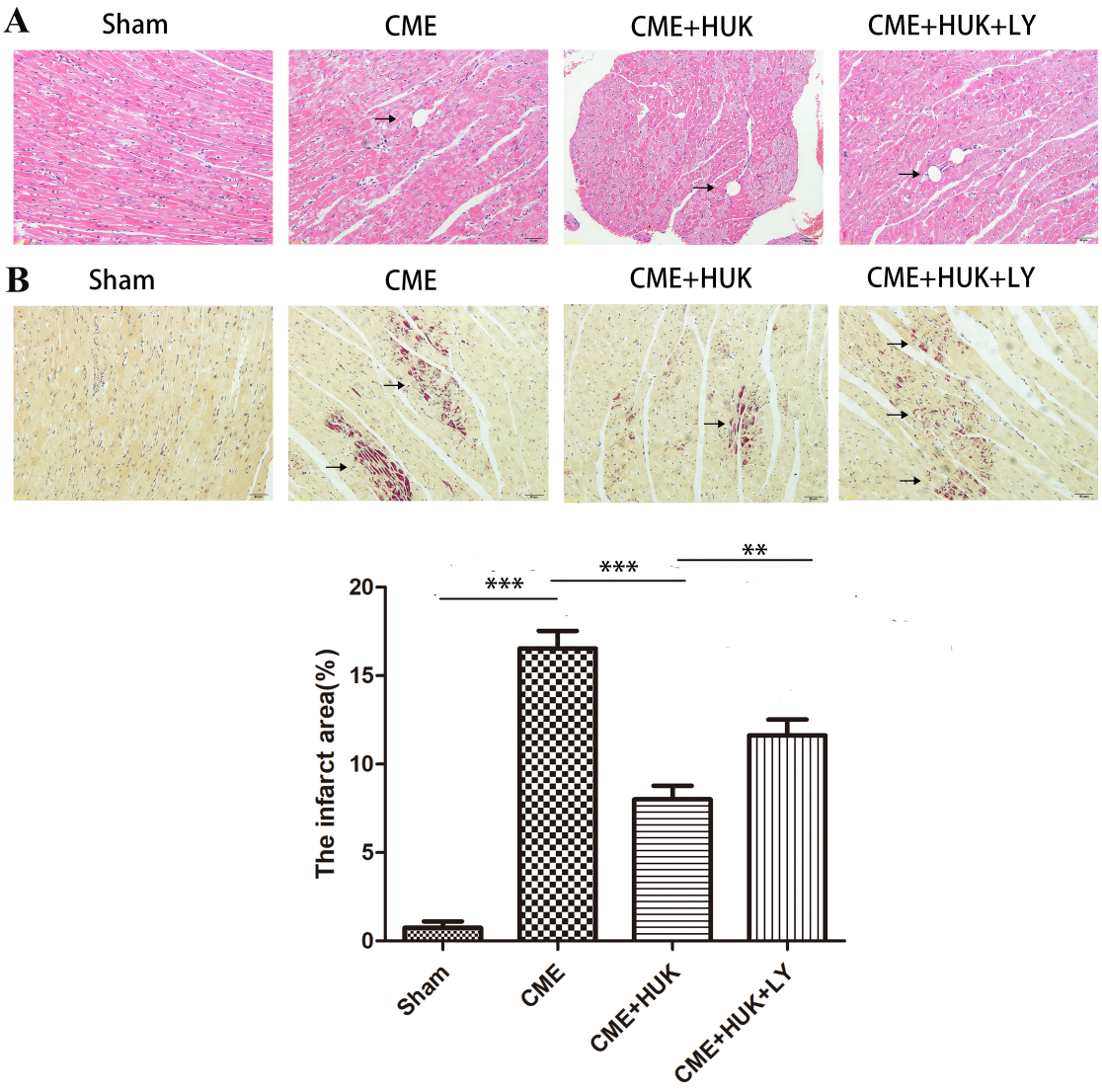

Fig. 3. H&E and HBFP staining of myocardial tissues (×200 magnification; bar = 50 μm) (n = 6, per group). (A) H&E staining. Microspheres were observed in the CME, CME + HUK, and CME + HUK + LY groups but not in the Sham group. The arrows indicated the microspheres. (B) HBFP staining. An ischemic myocardium was highlighted in red. Data were presented as the mean ± SD. *$p < 0.05$, **$p < 0.01$, ***$p < 0.001$. Abbreviations: CME, coronary microembolization; HUK, Human Urinary Kallidinogenase; LY, LY294002.

separating gel: 10–15% SDS-PAGE) was utilized to separate the total protein obtained from cardiac tissues and then transferred it to a polyvinylidene fluoride membrane (PVDF, Millipore, Atlanta, Georgia, United States). The above experimental operations were all completed at a constant voltage of 100 V. The membrane was then sealed with BSA at 25 °C for 1 hour. Next, the membrane was hatched with corresponding primary antibodies at 4 °C for 24 hours. After 24 hours, the membrane was washed five times. We then incubated the secondary antibody (ab6721, 1:10000, Abcam) coupled to the enzyme for 2 hours.

2.10 Statistical Analysis

All data were analyzed in SPSS software (version 23.0, IBM, Chicago, IL, USA). The results of our experiments are presented as mean standard deviation (SD). ANOVA was conducted to test the significance of differences in sample means, and a p-value < 0.05 was set as the threshold. Graphpad Prism software (version 8.0, San Diego, CA, USA) for data visualization.

3. Results

3.1 Effect of HUK on Cardiac Function of SD Rats

To assess circulatory changes in rats, we measured the LVEF, LVFS, LVEDd, and LVESd after 12 h in the CME model. The echocardiographic results of each group demonstrated that the CME group had lower LVEF and LVFS values than the Sham group, while LVEDd and LVESd were reversed (Fig. 2A,B). Additionally, cardiac

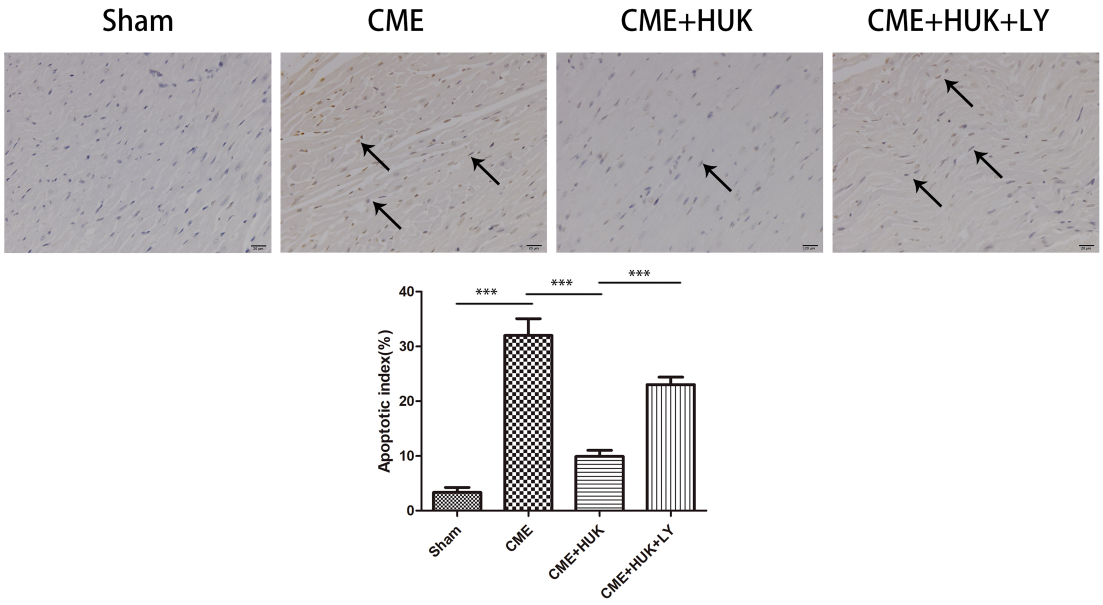

Fig. 4. TUNEL staining results of the infarcted and normal cardiomyocyte nuclei and the apoptosis rate of cardiomyocytes in each group (n = 6, per group). The arrows indicated the microspheres. The nuclei of normal cardiomyocytes were stained light blue, while apoptotic cardiomyocytes' nuclei were stained yellow-brown. Data were presented as the mean ± SD. *$p < 0.05$, **$p < 0.01$, ***$p < 0.001$. Abbreviations: CME, coronary microembolization; HUK, Human Urinary Kallidinogenase; LY, LY294002.

function was improved in the CME + HUK group compared with the CME group, showing higher LVEF/LVFS and lower LVEDd/LVESd.

3.2 Effect of HUK on the Microinfarct Size after CME

H&E and HBFP staining suggested that there were sporadic ischemic areas in the Sham group and most areas were normal filling tissues (Fig. 3A,B). In the CME, CME + HUK, and CME + HUK + LY groups, micro-infarct areas were observed; most of the infarct areas were located in the left ventricle, and embolized microspheres could be seen in the field of vision. The results of H&E staining indicated that cardiomyocytes in the micro-infarct area had no nuclei or ruptured nuclei; the cytoplasm was also red. In addition, the area around the infarct showed swelling and degeneration of cardiomyocytes, red blood cell effusion, and infiltration of inflammatory cells. The HBFP staining results showed that the infarct area of CME rats was significantly wider than that of the Sham group ($p < 0.05$). The infarct area in the CME group was also significantly wider than that of the CME + HUK group ($p < 0.05$).

3.3 Multi-Indicator Assessment of Apoptosis in Rat Cardiomyocytes

TUNEL staining results (Fig. 4) have distinguished infarcted and normal myocardial nuclei; we found that apoptotic cardiomyocytes were mainly distributed in the peri-infarct region of myocardial microinfarction. The apoptosis rate was dramatically higher in the CME group than in the Sham and CME + HUK groups (both $p < 0.05$), and LY294002 and HUK treatment balanced the anti-apoptotic function of HUK. Meanwhile, we assessed mRNA translation and protein levels using RT-qPCR and western blotting. RT-qPCR analysis (Fig. 5A) showed that the expression levels of caspase-3 and Bax in the myocardial tissue were significantly higher in the CME group than in the Sham and CME + HUK groups, and Bcl-2 was lower (both $p < 0.05$). Additionally, the expression levels of Bax and caspase-3 in cardiomyocytes in the CME + HUK + LY group were significantly higher than those in the CME + HUK group ($p < 0.05$). In contrast, the expression of Bcl-2 in the CME group was significantly downregulated ($p < 0.05$). Western blotting (Fig. 5B) results were concordant with RT-qPCR.

Furthermore, we observed from the IF results that Bax and cleaved caspase-3 expression levels were significantly decreased in the Sham and CME + HUK groups compared to those in the CME and CME + HUK + LY groups, and Bcl-2 in the CME and CME + HUK + LY groups were significantly downregulated (Fig. 6).

3.4 Effect of HUK on the Inflammation of Cardiomyocytes

To explore the effect of HUK on cardiomyocyte inflammation, two methods (ELISA and western blotting) were used to identify the relative expression levels of IL-1β and TNF-α in the different samples (Fig. 7). Interestingly, consistent results were obtained. Briefly, the measurement results of the aforementioned methods all indicated that the expression levels of IL-1β and TNF-α in the CME group were significantly higher than that of the Sham group. In addition, compared with the CME group, the expression levels of IL-1β and TNF-α in the CME + HUK group were significantly lower (both $p < 0.05$). The expression levels

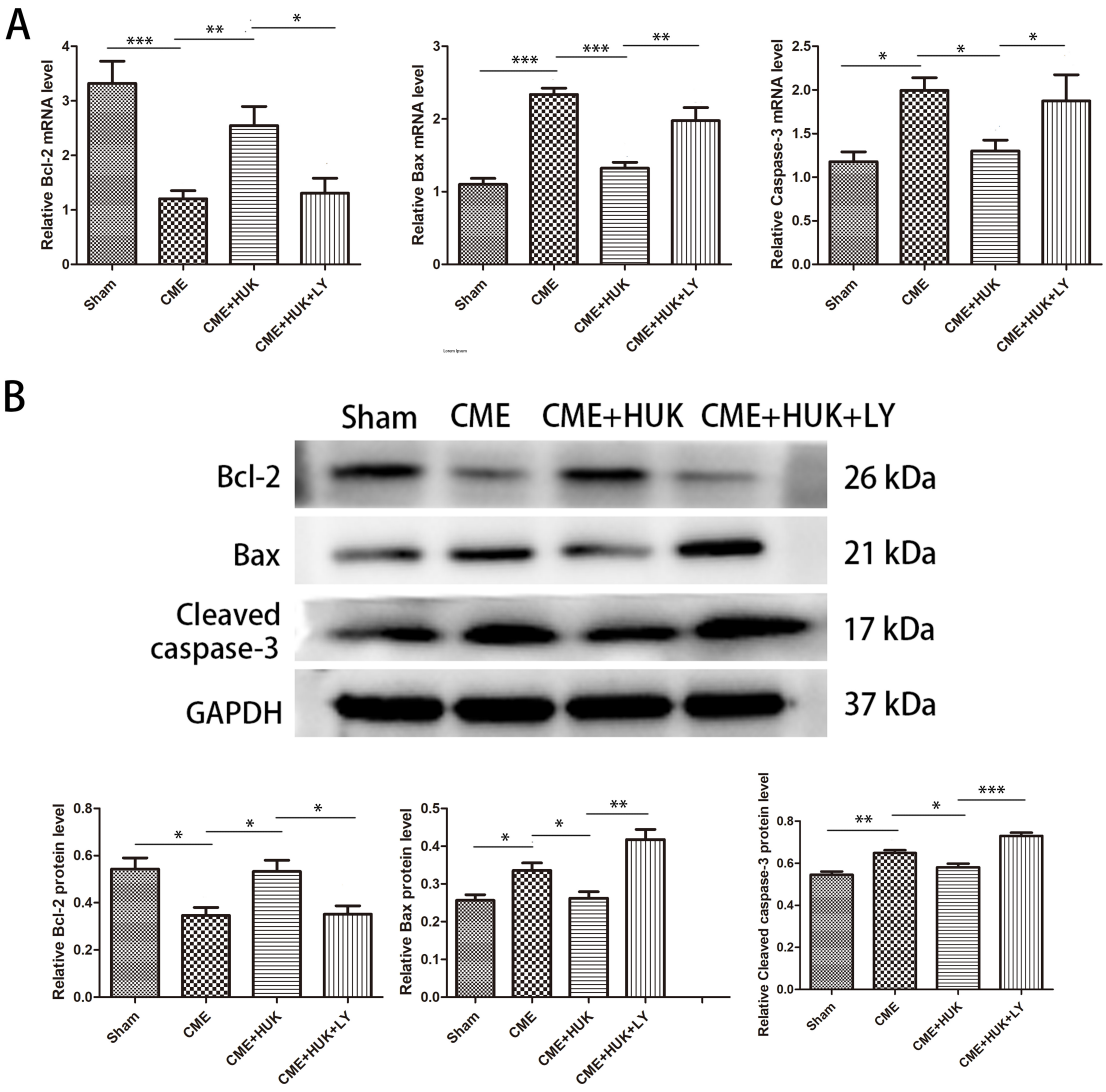

Fig. 5. Pretreatment with HUK attenuated CME-induced myocardial apoptosis. (A) The mRNA expression levels of Bcl-2, Bax, and caspase-3 in cardiac tissues (n = 6, per group). (B) The protein expression levels of Bcl-2, Bax, and cleaved caspase-3 in cardiac tissues (n = 3, per group). Data were presented as the mean ± SD. *$p < 0.05$, **$p < 0.01$, ***$p < 0.001$. Abbreviations: CME, coronary microembolization; HUK, Human Urinary Kallidinogenase; LY, LY294002.

of IL-1β and TNF-α in the CME + HUK + LY group were significantly higher than those in the CME + HUK group ($p < 0.05$).

3.5 Serum CK-MB/textbackslash cTnI/textbackslash LDH Levels

In this study, we quantified serum myocardial injury biomarkers (including cTnI, LDH, and CK-MB) between groups (Fig. 8A–C). Briefly, the degree of myocardial damage was assessed by calculating the serum cTnI, LDH, and CK-MB levels. The CME group had significantly higher serum levels of CK-MB, cTnI, and LDH compared to the Sham group. In addition, serum LDH, cTnI, and CK-MB levels in the CME + HUK group were significantly lower than those in the CME group. Compared with the CME + HUK group, serum CK-MB, cTnI, and LDH levels were significantly higher in the CME + HUK + LY group (all $p < 0.05$).

3.6 Effect of HUK on the PI3K/Akt/FoxO1 Signaling Pathway

Here, we determined the relative expression levels of PI3K/Akt/FoxO1 signaling pathway marker genes (p-PI3K, PI3K, p-Akt, Akt, p-FoxO1, and FoxO1) at the protein levels‘1 using western blotting (Fig. 9). This indicated that the expression levels of p-PI3K, p-Akt, and p-FoxO1 in the CME group were significantly lower than those in the Sham and CME + HUK groups (all $p < 0.05$). Compared to the CME + HUK group, the expression levels of p-PI3K, p-Akt, and p-FoxO1 in the CME + HUK + LY group were significantly lower (all $p < 0.05$). In addition, compared with the CME group, the rates of p-PI3K/PI3K, p-Akt/Akt,

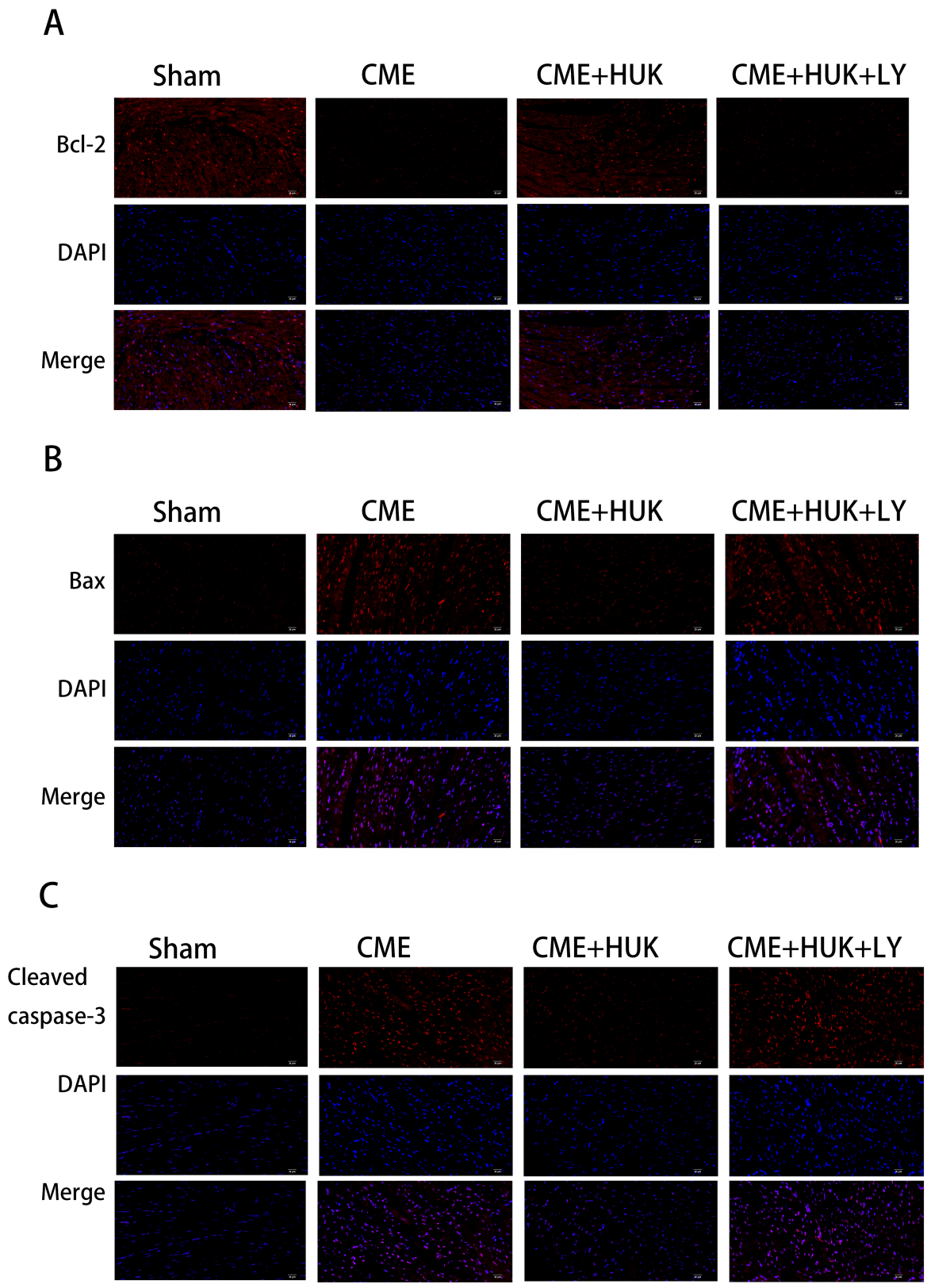

Fig. 6. Immunofluorescence staining of Bax, Bcl-2, and cleaved caspase-3 in cardiac tissues (magnification ×400, scale bar = 20 μm) (n = 3, per group). (A) IF staining detected the expression of Bcl-2. (B) IF staining detected the expression of Bax. (C) IF staining detected the expression of cleaved caspase-3. Abbreviations: CME, coronary microembolization; HUK, Human Urinary Kallidinogenase; LY, LY294002; IF, Immunofluorescence.

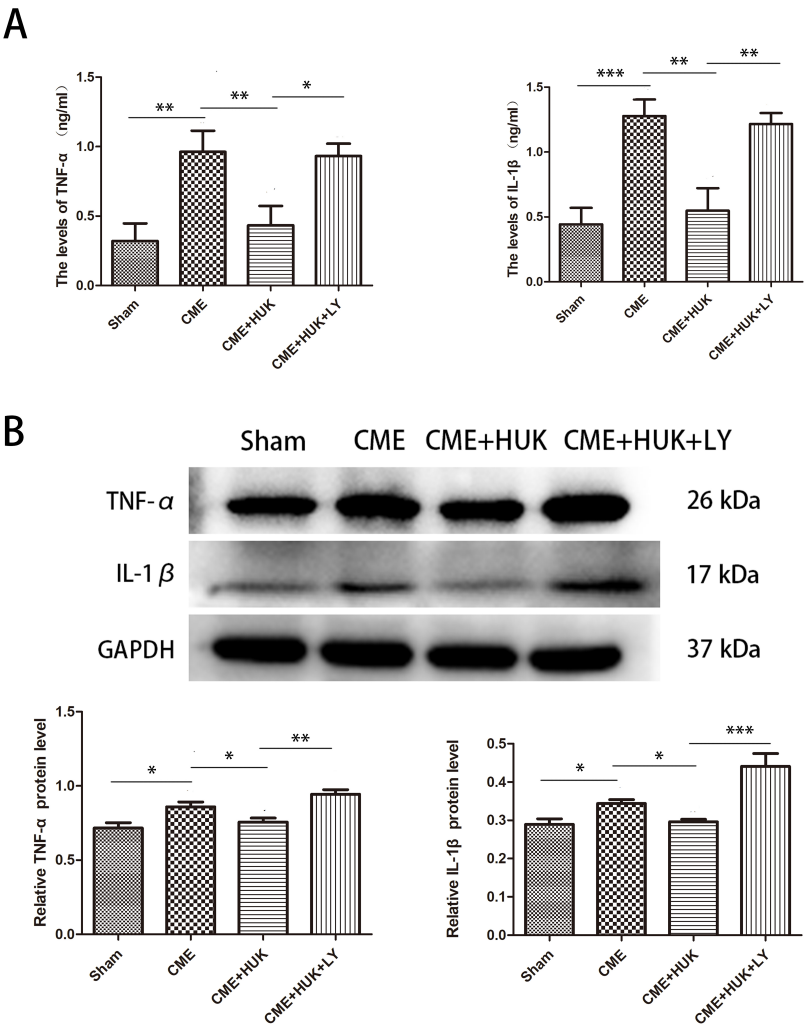

Fig. 7. Human Urinary Kallidinogenase reduced the myocardial inflammation. (A) The serum levels of TNF-α and IL-1β in the four groups (n = 6, per group). (B) The protein expression levels of TNF-α and IL-1β in the four groups (n = 3, per group). Data were presented as the mean ± SD. *$p < 0.05$, **$p < 0.01$, ***$p < 0.001$. Abbreviations: CME, coronary microembolization; HUK, Human Urinary Kallidinogenase; LY, LY294002.

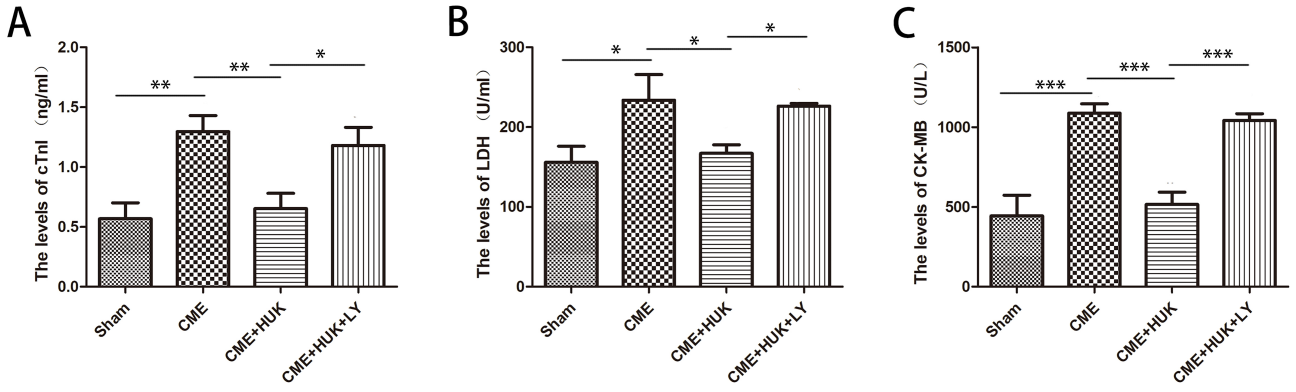

Fig. 8. Human Urinary Kallidinogenase reduced the serum levels of myocardial injury markers (n = 6 per group). (A) The blood levels of cTnI in the four groups. (B) The blood levels of LDH in the four groups. (C) The blood levels of CK-MB in the four groups. Data were presented as the mean ± SD. *$p < 0.05$, **$p < 0.01$, ***$p < 0.001$. Abbreviations: CME, coronary microembolization; HUK, Human Urinary Kallidinogenase; LY, LY294002.

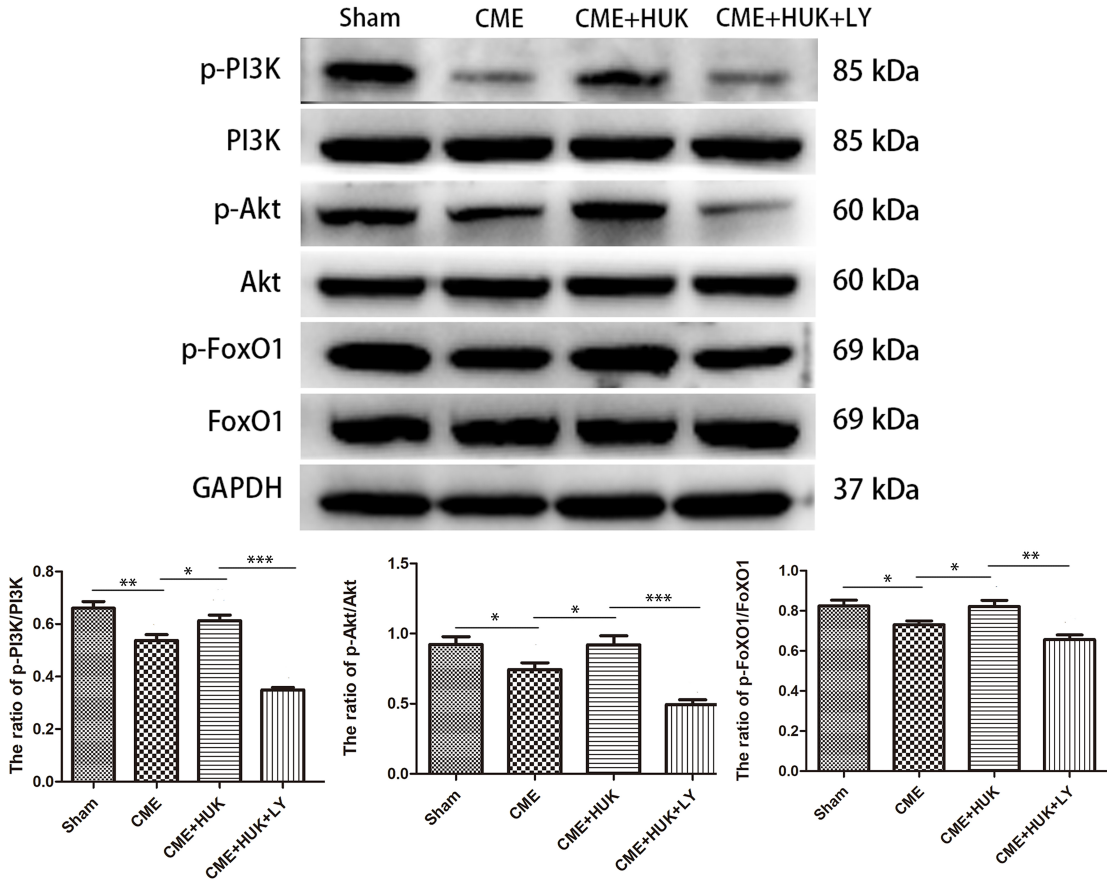

Fig. 9. Effect of HUK on PI3K/Akt/FoxO1-associated protein expression in cardiac tissues (n = 3, per group). Data were presented as the mean ± SD. *$p < 0.05$, **$p < 0.01$, ***$p < 0.001$. Abbreviations: CME, coronary microembolization; HUK, Human Urinary Kallidinogenase; LY, LY294002.

and p-FoxO1/FoxO1 in the Sham and CME + HUK groups were significantly higher (all $p < 0.05$). In addition, the levels of p-PI3K/PI3K, p-Akt/Akt, and p-FoxO1/FoxO1 were significantly lower in the CME + HUK + LY group than in the CME + HUK group ($p < 0.05$).

4. Discussion

CME is a major cause of "no recurrent flow" in occluded coronary arteries after interventional procedures. The incidence of CME during perioperative PCI is 15%–20%, and it is as high as 45% in high-risk patients. CME may cause postoperative "no flow" or "slow flow" and microcirculation dysfunction, which in turn may lead to myocardial ischemia, arrhythmia, heart failure, and other consequences [16]. Given its high incidence, it has been viewed as an independent predictor of heart disease and mortality [17]. The aim of this study was to investigate the underlying mechanisms of HUK on CME. Our findings revealed that HUK activation of the PI3K/Akt/FoxO1 axis caused myocardial inflammation inhibition and anti-apoptosis, with the endpoint of ameliorating CME-induced myocardial injury.

HUK is an extract from urine, which was designed to block the post-stroke inflammatory cascade and became a class I new drug in the USA [14]. Accumulating studies have shown that HUK was negatively associated with TGF-β1/Smad2/3 expression and positively associated with p-eNOS activity, thereby affecting endothelial epigenetics [18]. Moreover, HUK has been found to effectively inhibit inflammation and prevent ischemic brain damage by activating the MAPK/ERK pathway or downregulating the NF-κB pathway [19]. Han *et al.* [14] demonstrated that HUK had neuroprotective functions, including reducing the infarct size and improving neurological deficits by upregulating VEGF and the apelin/APJ pathway. Notably, the pathogenesis of the above-mentioned cerebrovascular diseases has commonalities with the pathogenesis of CME. Therefore, existing research has shown that HUK may have promising research prospects in managing CME.

The PI3K/Akt signaling pathway is associated with the regulation of physiological functions such as apoptosis and inflammation. Its activation can reduce myocardial apoptosis and inflammation, thereby effectively reducing myocardial damage [20–22]. PI3K/Akt signaling pathway has mediated various biomolecules, including rapamycin (mTOR), glycogen synthase kinase 3 (GSK-3), forkhead

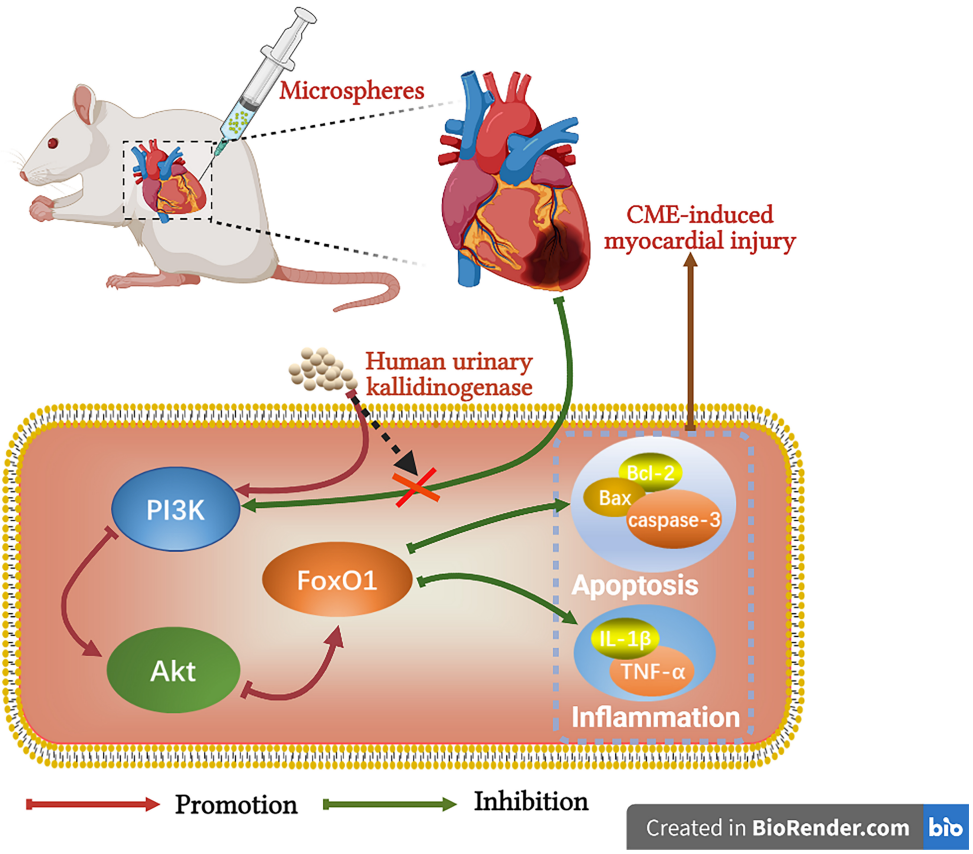

Fig. 10. Mechanism chart of HUK exerting cardioprotective effect in CME through PI3K/Akt/FoxO1 axis, created with BioRender (https://biorender.com/). Abbreviations: CME, coronary microembolization; HUK, Human Urinary Kallidinogenase.

box protein O1/3 (FoxO1/3), and nitric oxide synthase (NOS) [23]. He *et al*. [12] concluded that lipopolysaccharide located in the PI3K/Akt/FoxO1 pathway were beneficial to neuronal cell development, including injury mitigation, inhibition of apoptosis, and protection [24]. HUK was found to reduce apoptosis and inflammation in acute ischemic stroke by activating the PI3K/AKT/FoxO1 axis, thereby playing a protective role against brain injury. However, the effects of HUK on the PI3K/Akt/FoxO1 axis in CME and its role in CME have not been thoroughly studied.

Our previous studies showed that CME usually leads to cardiomyocyte apoptosis and inflammation, which may cause cardiac dysfunction [6,25]. For cardiomyocyte apoptosis, the previous studies demonstrated substantial cardiomyocyte apoptosis and abnormal expression of apoptosis-related genes (up-regulated Bax and Cleaved caspase-3; down-regulated Bcl-2) in the infarct zone [26, 27]. For cardiomyocyte inflammation, the expression levels of inflammation-related genes (IL-1β and TNF-α) in the CME group were significantly upregulated compared with those in the Sham group [28,29]. These results are consistent with those obtained in this study, which provides a level of credibility.

We found that CME caused inflammation and increased apoptosis in rat cardiomyocytes, leading to severe myocardial damage. HUK (pretreatment starting 7 days before CME) was involved in activating the PI3K/Akt/FoxO1 axis and decreasing myocardial inflammation and apoptosis, thereby exerting a cardioprotective effect in CME (shown in Fig. 10). In contrast, when treated CME with the PI3K specific inhibitor LY294002, the essential proteins p-PI3K, p-Akt, and p-FoxO1 were significantly downregulated, indicating that the PI3K/Akt/FoxO1 signaling pathway was suppressed. The expression levels of inflammation-related genes (IL-1β and TNF-α) and pro-apoptotic genes (Bax and cleaved caspase-3) increased significantly, while that of Bcl-2 decreased. Thus, the cardioprotective effect of HUK was reduced by the application of LY294002.

This study had a few limitations. Firstly, the plastic microspheres of the CME rat model were not equipped with biological characteristics for atherosclerotic plaques (thrombosis, vasoactivity), and could not be equated with clinicopathological changes. Secondly, we investigated the effect of HUK on the inhibition of myocardial inflammation and apoptosis induced by CME through the PI3K/Akt/FoxO1 signalling pathway. However, we only used the PI3K specific inhibitor (LY294002) to affect the PI3K/Akt/FoxO1 signalling pathway. PI3K downstream

molecules must also be targeted to exclude specificity further and avoid serendipity. Finally, other signalling pathways may be involved; therefore, further *in vitro*, or *in vitro* studies are required.

5. Conclusions

In summary, the findings of this study identified that HUK antagonizes CME-induced myocardial injury and exerts substantial protection. These cardioprotective effects were mediated by the activation of the PIK/Akt/FoxO1 axis, which significantly inhibited myocardial inflammation and apoptosis. Therefore, we speculated that HUK could potentially be used clinically in the "golden time" of CME and pretreatment. This research has the potential to provide a certain reference value for novel ideas in HUK, which would guide CME-related clinical strategies.

Data Sharing Statement

The data used to support the findings of this study are available from the corresponding author upon request.

Author Contributions

LL and JX conceived the project; JX and BHM designed the study; TL and BHM directed the study; YQX, JX, BLW drafted the manuscript; YHL, GQL and QQN was responsible for all data analysis; LL, JX revised the manuscript; All authors have read and agreed to the published version of the manuscript.

Ethics Approval and Consent to Participate

Animal experimental protocols and steps in our study according to the NIH Guidelines for the Use of Laboratory Animals and were approved by the Animal Ethics Committee of Guangxi Medical University (License number: 202101006).

Acknowledgment

This work was supported by the First Affiliated Hospital of Guangxi Medical University.

Funding

This work was supported by Innovative Research Team Projec of Guangxi Natural Science Foundation (Grant No. 2018GXNSFGA281006) & the National Natural Science Foundation of China (Grant No. 82170349).

Conflict of Interest

The authors declare no conflict of interest.

References

[1] Chen A, Chen Z, Xia Y, Lu D, Jia J, Hu K, *et al.* Proteomics Analysis of Myocardial Tissues in a Mouse Model of Coronary Microembolization. Frontiers in Physiology. 2018; 9: 1318.

[2] Su Q, Li L, Liu Y, Zhou Y, Wen W. Effect of metoprolol on myocardial apoptosis after coronary microembolization in rats. World Journal of Emergency Medicine. 2013; 4: 138.

[3] Mo B, Wu X, Wang X, Xie J, Ye Z, Li L. MiR-30e-5p Mitigates Hypoxia-Induced Apoptosis in Human Stem Cell-Derived Cardiomyocytes by Suppressing Bim. International Journal of Biological Sciences. 2019; 15: 1042–1051.

[4] Chen ZQ, Zhou Y, Chen F, Huang JW, Zheng J, Li HL, *et al*. Breviscapine Pretreatment Inhibits Myocardial inflammation and apoptosis in Rats After Coronary Microembolization by Activating the PI3K/Akt/GSK-3beta Signaling Pathway. Drug Design, Development and Therapy. 2021; 15: 843–855.

[5] Heusch G, Skyschally A, Kleinbongard P. Coronary microembolization and microvascular dysfunction. International Journal of Cardiology. 2018; 258: 17–23.

[6] Chen ZQ, Zhou Y, Huang JW, Chen F, Zheng J, Li HL, *et al*. Puerarin pretreatment attenuates cardiomyocyte apoptosis induced by coronary microembolization in rats by activating the PI3K/Akt/GSK-3beta signaling pathway. The Korean Journal of Physiology & Pharmacology. 2021; 25: 147–157.

[7] Liu Y, Liu Y, Huang X, Zhang J, Yang L. Protective effects and mechanism of curcumin on myocardial injury induced by coronary microembolization. Journal of Cellular Biochemistry. 2019; 120: 5695–5703.

[8] Wang J, Chen H, Su X, Zhou Y, Li L. Atorvastatin Pretreatment Inhibits Myocardial Inflammation and Apoptosis in Swine after Coronary Microembolization. Journal of Cardiovascular Pharmacology and Therapeutics. 2017; 22: 189–195.

[9] Su Q, Li L, Zhao J, Sun Y, Yang H. Effects of nicorandil on PI3K/Akt signaling pathway and its anti-apoptotic mechanisms in coronary microembolization in rats. Oncotarget. 2017; 8: 99347–99358.

[10] Su Q, Lv X, Ye Z. Ligustrazine Attenuates Myocardial Injury Induced by Coronary Microembolization in Rats by Activating the PI3K/Akt Pathway. Oxidative Medicine and Cellular Longevity. 2019; 2019: 1–10.

[11] Han D, Chen X, Li D, Liu S, Lyu Y, Feng J. Human Urinary Kallidinogenase decreases recurrence risk and promotes good recovery. Brain and Behavior. 2018; 8: e01033.

[12] Ma N, Zhao Z, Zhang N, Chen H. Intra-arterial human urinary kallidinogenase alleviates brain injury in rats with permanent middle cerebral artery occlusion through PI3K/AKT/FoxO1 signaling pathway. Brain Research. 2018; 1687: 129–136.

[13] Lin Y, Huang G, Jin Y, Fang M, Lin D. Effects and mechanism of urinary kallidinogenase in the survival of random skin flaps in rats. International Immunopharmacology. 2019; 74: 105720.

[14] Han L, Li J, Chen Y, Zhang M, Qian L, Chen Y, *et al*. Human Urinary Kallidinogenase Promotes Angiogenesis and Cerebral Perfusion in Experimental Stroke. PLoS ONE. 2015; 10: e0134543.

[15] Li T, Chen Z, Zhou Y, Li H, Xie J, Li L. Resveratrol Pretreatment Inhibits Myocardial Apoptosis in Rats Following Coronary Microembolization via Inducing the PI3K/Akt/GSK-3β Signaling Cascade. Drug Design, Development and Therapy. 2021; 15: 3821–3834.

[16] Sun YH, Su Q, Li L, Wang XT, Lu YX, Liang JB. Expression of p53 in myocardium following coronary microembolization in rats and its significance. Journal of Geriatric Cardiology. 2017; 14: 292–300.

[17] Bikou O, Tharakan S, Yamada KP, Kariya T, Gordon A, Miyashita S, *et al*. A Novel Large Animal Model of Thrombogenic Coronary Microembolization. Frontiers in Cardiovascular Medicine. 2019; 6: 157.

[18] Lan W, Yang F, Li Z, Liu L, Sang H, Jiang Y, *et al*. Human urine kininogenase attenuates balloon-induced intimal hyperplasia in rabbit carotid artery through transforming growth factor beta1/Smad2/3 signaling pathway. Journal of Vascular Surgery. 2016; 64: 1074–1083.

[19] Chen ZB, Huang DQ, Niu FN, Zhang X, Li EG, Xu Y. Human urinary kallidinogenase suppresses cerebral inflammation in experimental stroke and downregulates nuclear factor-kappaB. Journal of Cerebral Blood Flow and Metabolism. 2010; 30: 1356–1365.

[20] Dhanasekaran A, Gruenloh SK, Buonaccorsi JN, Zhang R, Gross GJ, Falck JR, *et al*. Multiple antiapoptotic targets of the PI3K/Akt survival pathway are activated by epoxyeicosatrienoic acids to protect cardiomyocytes from hypoxia/anoxia. American Journal of Physiology-Heart and Circulatory Physiology. 2008; 294: H724–H735.

[21] Ebner B, Lange SA, Hollenbach D, Steinbronn N, Ebner A, Fischaleck C, *et al*. In Situ Postconditioning with Neuregulin-1β is Mediated by a PI3K/Akt-Dependent Pathway. Canadian Journal of Cardiology. 2015; 31: 76–83.

[22] Cortés-Vieyra R, Bravo-Patiño A, Valdez-Alarcón JJ, Juárez MC, Finlay BB, Baizabal-Aguirre VM. Role of glycogen synthase kinase-3 beta in the inflammatory response caused by bacterial pathogens. Journal of Inflammation. 2012; 9: 23.

[23] Qin W, Cao L, Massey IY. Role of PI3K/Akt signaling pathway in cardiac fibrosis. Molecular and Cellular Biochemistry. 2021; 476: 4045–4059.

[24] He F, Zhang N, Lv Y, Sun W, Chen H. Low-dose lipopolysaccharide inhibits neuronal apoptosis induced by cerebral ischemia/reperfusion injury via the PI3K/Akt/FoxO1 signaling pathway in rats. Molecular Medicine Reports. 2019; 19: 1443–1452.

[25] Kretzschmar D, Jung C, Otto S, Utschig S, Hartmann M, Lehmann T, *et al*. Detection of coronary microembolization by Doppler ultrasound in patients with stable angina pectoris during percutaneous coronary interventions under an adjunctive antithrombotic therapy with abciximab: design and rationale of the High Intensity Transient Signals ReoPro (HITS-RP) study. Cardiovascular Ultrasound. 2012; 10: 21.

[26] Yuan Y, Li B, Peng W, Xu Z. Protective effect of glycyrrhizin on coronary microembolization-induced myocardial dysfunction in rats. Pharmacology Research Perspectives. 2021; 9: e00714.

[27] Mao Q, Liang X, Wu Y, Lu Y. Resveratrol Attenuates Cardiomyocyte Apoptosis in Rats Induced by Coronary Microembolization through SIRT1-Mediated Deacetylation of p53. Journal of Cardiovascular Pharmacology and Therapeutics. 2019; 24: 551–558.

[28] Su Q, Li L, Sun Y, Yang H, Ye Z, Zhao J. Effects of the TLR4/Myd88/NF-κB Signaling Pathway on NLRP3 Inflammasome in Coronary Microembolization-Induced Myocardial Injury. Cellular Physiology and Biochemistry. 2018; 47: 1497–1508.

[29] Li L, Li D, Qu N, Wen W, Huang W. The Role of ERK1/2 Signaling Pathway in Coronary Microembolization-Induced Rat Myocardial Inflammation and Injury. Cardiology. 2010; 117: 207–215.